

Neuroimaging of cerebral activations and deactivations associated with hypercapnia and hunger for air

Stephen Brannan^{*†}, Mario Liotti^{*}, Gary Egan[‡], Robert Shade[§], Lisa Madden[§], Rachel Robillard[¶], Bart Abplanalp[¶], Katie Stofer^{*}, Derek Denton[‡], and Peter T. Fox^{*}

^{*}Research Imaging Center, Medical School, University of Texas Health Science Center, Floyd Curl Drive, San Antonio, TX 78284; [†]Howard Florey Institute of Experimental Physiology and Medicine, University of Melbourne, Victoria 3010, Australia; [‡]Southwest Foundation for Biomedical Research, P. O. Box 760549, San Antonio, TX 78245-0549; and [¶]Departments of Psychology and Educational Psychology, University of Texas, Austin, TX 78712

Contributed by Derek Denton, December 18, 2000

There are defined medullary, mesencephalic, hypothalamic, and thalamic functions in regulation of respiration, but knowledge of cortical control and the elements subserving the consciousness of breathlessness and air hunger is limited. In nine young adults, air hunger was produced acutely by CO₂ inhalation. Comparisons were made with inhalation of a N₂/O₂ gas mixture with the same apparatus, and also with paced breathing, and with eyes closed rest. A network of activations in pons, midbrain (mesencephalic tegmentum, parabrachial nucleus, and periaqueductal gray), hypothalamus, limbic and paralimbic areas (amygdala and periamygdalar region) cingulate, parahippocampal and fusiform gyrus, and anterior insula were seen along with caudate nuclei and pulvinar activations. Strong deactivations were seen in dorsal cingulate, posterior cingulate, and prefrontal cortex. The striking response of limbic and paralimbic regions points to these structures having a singular role in the affective sequelae entrained by disturbance of basic respiratory control whereby a process of which we are normally unaware becomes a salient element of consciousness. These activations and deactivations include phylogenetically ancient areas of allocortex and transitional cortex that together with the amygdalar/periamygdalar region may subserve functions of emotional representation and regulation of breathing.

Regulatory physiologic processes occur continuously beyond the realm of consciousness, and only rarely do we volitionally attend to them or do they intrude and dominate conscious awareness. Feeling breathless or “hunger for air” is one process capable of making such an imperious intrusion. Intense breathlessness occurs in certain psychiatric states such as panic disorder (theorized to be due to a malfunction of the “suffocation alarm”) (1), where no physiologic impairment accounts for the reaction. This fact indicates the involvement of higher brain centers, and that basic respiratory circuitry can be accessed and powerfully influenced by neural processes subserving emotion.

Humans are extremely sensitive to carbon dioxide. The pathway for this effect involves pH changes (2) detected by the neurons of the ventral respiratory group. How this sensitivity leads to respiratory changes and the perception of air hunger has been explored in humans by elegant work by Banzett and colleagues (3, 4), and Gandevia and colleagues (5). Their work, including study of curarized subjects and quadriplegics, indicates that central neural processes are involved in the perception of air hunger and that peripheral afferents play a minor role.

The CO₂-sensitive neurons in the ventral respiratory group and Botzinger complexes, aligned along the ventrolateral medulla, are involved in generating respiratory rhythms. Studies in rats using anterograde and retrograde tracing of connections of the ventral respiratory group show widespread projections involving several cerebellar regions, brainstem, midbrain, hypothalamus, thalamus, amygdalohippocampal area, and insula in a putative network (6). Also, the caudal hypothalamus modulates respiratory response to inhalation of increased levels of CO₂ (7). A functional MRI study

in humans using 5% CO₂ in steady-state inhalation versus 100% O₂ inhalation found involvement of the ventral and dorsal medulla, midline pons, and midline cerebellum (8).

Other human neuroimaging work with positron emission tomography (PET) and functional MRI has examined the volitional control of breathing, showing consistent activations of primary motor, primary sensory, and premotor areas (9, 10). In another study, 5% CO₂ inhalation was contrasted to passive isocapnic ventilation. The majority of subjects reported breathlessness in the CO₂ trials. There were activations in brainstem and hypothalamus, and in hippocampus, anterior cingulate and fusiform gyrus and anterior insula, suggesting a participation of the limbic system in hypercapnia and air hunger (11). These effects were explained by the unpleasantness of the sensation of air hunger or by a direct effect of CO₂ (11, 12).

The goal of the present study was to better elucidate the interaction between the basic respiratory circuitry and the central cortical/limbic control of breathing during CO₂-induced air hunger. Rapid onset, transient states of intense breathlessness (*ca.* 8% CO₂ inhalation) were contrasted to periods of breathing an N₂/O₂ mixture [both using a facemask (FM)], to periods of voluntary paced breathing (PB) of room air (hyperventilation), and to regular spontaneous breathing of room air (rest). The main focus of the study was to identify the midbrain, hypothalamic, limbic, and cortical networks associated with CO₂ stimulation and hunger for air. The contrasts aimed to minimize the effects of confounding factors such as the respiratory apparatus and associated stimulation, increased respiratory rate, and anticipatory anxiety. Thus the present paper deals with the regional cerebral blood flow (rCBF) changes caused by the combination of hypercapnia and air hunger. The effects attributable solely to air hunger, and the changes observed in the cerebellum will be the subject of separate papers.

Methods

Subject Recruitment. From a group of 60 subjects prescreened with a 5-min trial of CO₂, nine subjects were selected who had low anxiety (as measured by the Anxiety Sensitivity Index), a robust breathlessness response to the CO₂, and easily tolerated the procedure. The nine healthy right-handed subjects (six males, three females; age range 22 to 42, mean age 28 ± 6 years) gave written informed consent; the study was conducted as approved by the Institutional Review Board of the University of Texas Health Sciences Center at San Antonio. All subjects engaged in moderate

Abbreviations: PET, positron emission tomography; FM, facemask; CBF, cerebral blood flow; rCBF, regional CBF; gCBF, global CBF; PB, paced breathing; MP, mouthpiece; BA, Brodmann's area; PCO₂, partial pressure CO₂; ACC, anterior cingulate cortex.

[†]To whom reprint requests should be addressed: E-mail: brannan@uthscsa.edu.

The publication costs of this article were defrayed in part by page charge payment. This article must therefore be hereby marked “advertisement” in accordance with 18 U.S.C. §1734 solely to indicate this fact.

Table 1. Gas composition and inhalation method for each of the six experimental conditions

Condition name	Gas composition	Administration	Respiration rate	Condition code	Scans/subject
CO ₂ FM	8% CO ₂ , 92% O ₂	FM	Involuntarily high	CO ₂ FM	2
CO ₂ MP	8% CO ₂ , 92% O ₂	MP	Involuntarily high	CO ₂ MP	2
PB	79% N ₂ , 21% O ₂	FM	Voluntarily high	PB FM	1
PB	79% N ₂ , 21% O ₂	MP	Voluntarily high	PB MP	1
O ₂ FM	9% N ₂ , 91% O ₂	FM	Normal	O ₂ FM	2
Eyes closed rest	79% N ₂ , 21% O ₂	None	Normal	R	2

physical activity at least weekly, and none was an athlete with protracted and daily anaerobic training.

Respiratory Procedures and Analysis. Inspired gases were provided by an open circuit consisting of a FM (Hudson RCI Air Cushion mask no. 1276, Temecula, CA) or a mouthpiece (MP) attached to a tee connector with one-way valves to regulate the direction of the inspired and expired gases. During all experiments a respiratory gas monitor (Ohmeda 5250 Respiratory Gas Monitor, Ohmeda, Madison, WI), measured inspired partial pressure CO₂ (PCO₂), end tidal PCO₂, respiratory rate, tidal volume, minute volume, oxygen saturation, and heart rate. Ventilator flow signals for this monitor were provided by a pneumotachometer attached to the outflow side of the circuit. A 7-liter bag was attached to the inflow side for regulating inspired gas composition via 25-mm diameter tubing. It was charged with a 9% CO₂, 91% O₂ gas mixture, which contrived delivery of 7.8% CO₂ to the FM. Inspired and expired gas was measured by attaching the sampling tubing for the gas monitor to a port provided on the tee connector. All variables were measured every 10 s and recorded by a computer connected to the RS-232 output of the respiratory gas monitor.

The main focus of this paper is the comparison between carbon dioxide inhalation using a FM (8% CO₂ + 92% O₂) (CO₂ FM) and oxygen inhalation using a FM (9% N₂ + 91% O₂) (O₂ FM). This comparison minimizes effects attributable to the apparatus used. In addition, the subjects were unaware of which gas mixture they would receive, and therefore any anticipatory arousal and anxiety were common to both. CO₂ FM also was compared with the PB condition to control for respiratory rate effects, and to the eyes closed rest condition (rest) as a baseline condition. Because our main focus was on producing intense air hunger, we concentrated on how to optimize the stimulus effects and so used a higher concentration of CO₂ (8%) than previously used by others (8). The concentration of CO₂ was chosen after extensive testing on investigators and subjects with CO₂ concentrations varying from 5% to 12%.

Physiological Monitoring. The measures of respiratory function allowed for the correct commencement of PET scanning and verification that physiological indices returned to baseline after each scan. PET scanning began *ca.* 3 min after commencement of CO₂ administration. After each scan a questionnaire was read to the subjects, asking them to rate on a scale from 0 to 100 various physical sensations, most importantly breathlessness/air hunger (but also lightheadedness, dizziness, sense of being smothered, anxiety, euphoria). Subjects also were asked for presence and intensity of other symptoms, if any.

Imaging Procedures. Ten PET scans were acquired for each subject. Two scans each were acquired of CO₂ inhalation via MP (CO₂ MP), CO₂ inhalation via FM, O₂ inhalation via FM, and at rest. One scan was acquired with PB via a MP and one with PB via FM (Table 1). Each subject was supine with their head supported in an hemicylindrical head holder, with eyes closed and in a quiet room. An i.v. cannula was inserted into the left forearm for injection of each H₂

¹⁵O bolus. The scanning methods used at the Imaging Center, University of Texas Health Science Center have been described (13–16). High-resolution MRI scans also were acquired for each subject. PET and anatomical MR images of each subject were coregistered and spatially normalized by using an affine, nine-parameter algorithm (16). Images were normalized to Talairach space (16, 17) and referenced in millimeters relative to the anterior commissure. A gamma 2 statistic measuring kurtosis of the histogram of the difference images (change distribution curve) (18) was calculated. This was followed by a maxima or minima search to identify local extrema within a search volume of 125 mm³ (19). Omnibus tests to assess overall significance then were performed on such extrema. This approach uses an empirical estimate of the independent elements in the subtraction image (resels), which is specifically computed for each subtraction image rather than simply estimated on theoretical number of independent voxels (20, 21). Anatomical labels were applied automatically by using a three-dimensional electronic brain atlas (22). Regions of rCBF change having statistical significance ($Z > 4.0$; cluster sizes > 45 voxels) are reported for the CO₂ FM primary comparison, and ($Z > 3.11$; cluster size > 45 voxels) for the secondary comparisons (e.g., PB versus rest). CO₂ effects on global CBF (gCBF) are well established, and thus we did not deem it justified to collect arterial blood samples for absolute gCBF quantification. However, relative gCBF was determined by summation of the radioactivity counts within the common brain volume of the nine subjects for each scan, normalized for injected radioactivity.

Limited Field of View. Given the limited field of view of the PET scanner (15 planes spanning 10 cm), our scans did not cover the entire brain and missed superior posterior parietal, posterior inferior cerebellum, and caudal medulla. Earlier studies, with comparable scanner field of view, and with interests in motor function, have positioned subjects higher in the scanner and therefore missed some of the findings we are reporting in the lower brain areas.

Results

Respiratory. The respiratory data from one of the subjects had to be discarded due to respiratory equipment errors. The group mean physiological results for the remaining eight subjects are presented for each condition (Table 2). Because the baseline levels immediately before each scan were similar for all conditions, the results have been averaged. Respiratory data from the two PB conditions (FM and MP) were averaged in the table. Mean values for the minute volume, end tidal PCO₂, and heart rate were entered into pairwise repeated measures ANOVA (superanova) with the factor of interest being the gas composition (CO₂ FM, O₂ FM, PB).

As expected (Table 2), end tidal PCO₂ was higher in the CO₂ FM relative to both the PB ($P < 0.0001$) and O₂ FM ($P < 0.0001$), but it was lower in the PB than in the O₂ FM condition ($P < 0.001$). Minute volume was greater during the CO₂ FM than during the O₂ FM ($P < 0.0001$) or PB ($P < 0.0001$). The minute volume was also smaller during the O₂ FM condition compared with the PB condition ($P = 0.03$). Heart rate during CO₂ FM and PB was significantly higher than during the O₂ FM condition ($P < 0.01$ and

Table 2. Group mean respiratory results (\pm SEM) for the eight subjects

Condition	Insp CO ₂ (%)	Exp CO ₂ (%)	Resp. rate (min ⁻¹)	Tidal volume (liters)	Min vent (liters/min)	Heart rate (min ⁻¹)	Breathlessness
Rest	0.10 (<0.01)	5.4 (0.1)***	11 (0.2)	0.72 (0.05)	6.2 (0.2)***	67 (1)*	0***
CO ₂ FM	7.80 (0.3)	8.8 (0.1)	15 (0.6)	1.51 (0.19)	22.7 (3.0)	78 (3)	73 (5)
O ₂ FM	0.10 (<0.01)	5.2 (0.2)***	10 (1)	0.75 (0.16)	6.6 (1.4)**	62 (2)*	5 (3)***
PB FM & MP	0.20 (0.01)	4.5 (0.3)***	19 (1)	0.57 (0.11)	10.3 (1.9)**	70 (4)	10 (4)***

Significance of difference of the rest, O₂ FM, and PB conditions relative to CO₂ FM: *, $P < 0.01$; **, $P < 0.001$; ***, $P < 0.0001$.

$P < 0.02$, respectively), but they were not significantly different from each other ($P = 0.12$). Recovery after a trial run was rapid (within 30–60 s) no matter what the gas composition or inhalation method.

Behavioral Results. The breathlessness ratings after the CO₂ FM condition (78 ± 3) were greater than following O₂ scans (5 ± 3) and PB scans (10 ± 4), confirming that the CO₂ inhalation was effective in producing air hunger. The CO₂ FM trials produced variable mild lightheadedness and faintness. Other sporadic reactions were a sense of smothering, mild euphoria, a transient mild headache, and dry throat. There was no tingling of the extremities or other sensory paresthesias, nausea, or gustatory or olfactory sensations.

PET Results. The results of the CO₂ FM condition compared with the CO₂ MP condition are reported separately, as are the results observed in the cerebellum for all of the comparisons.

Fig. 1 and Table 3 together show the rCBF increases during CO₂ FM compared with O₂ FM, PB, and rest [omnibus significance, two-tailed: CO₂ FM vs. O₂ FM total number of independent extrema (NIE) = 521, Z score = 3.17, $P = 0.00077$; CO₂ FM vs. PB: NIE = 472, Z score = 3.16, $P = 0.000079$; CO₂ FM vs. rest: NIE = 501, Z score = 3.22, $P = 0.00063$].

A similar pattern of activations and deactivations was observed with CO₂ FM independently of which control state was used for

comparison. Significant clusters were found in the midbrain (periaqueductal gray and pons), in the hypothalamus, in the amygdala and periamygdalar regions, hippocampus [Brodmann's area 28 (BA28)] and parahippocampal regions (BA20 and BA36), subgenual anterior cingulate cortex (ACC) (BA24), fusiform gyri (BA36), and several sites in midline and lateral cerebellum.

Fig. 1 and Table 3 show the similar rCBF decreases during CO₂ FM independently of which control state was used for comparison. These include dorsal ACC, posterior cingulate cortex (BA 31/23), dorsal prefrontal cortex (BA8/9), and ventral prefrontal cortex (BA11 and BA10).

Other effects. Activations in insular cortex and right pulvinar were present only for the contrasts CO₂ FM versus O₂ FM, and CO₂ FM versus rest. Activations of the caudate and putamen were primarily observed for CO₂ FM versus O₂ FM. Overall, all effects were observed in the three comparisons when using a lower Z -score significance threshold, with the exception of the anterior insular activations, which were not present in the CO₂ FM versus PB contrast.

Motor effects. Fig. 2 shows the motor activations during the PB versus rest comparison (omnibus significance: $\beta-1 = 2.4$, $df = 2180$, $P = 0.017$, two-tailed). Activation of primary motor cortex (precentral BA4, or M1-mouth) and premotor cortex (inferior precentral BA6) was observed in the comparison of PB versus rest (Fig. 2a); omnibus significance: number of independent extrema = 636, Z score = 4.33, $P = 0.00003$, two-tailed. Importantly, these effects were exactly matched by inverse sign changes (relative deactivations) in the CO₂ FM versus PB comparison.

gCBF changes. gCBF increases were observed for the CO₂ FM condition as expected. Compared with the rest condition, the relative gCBF increase was 21%, whereas for the O₂ FM and PB conditions the relative gCBF decreases were 5% and 19%, respectively.

Discussion

CO₂ inhalation succeeded in producing substantial rapid respiratory responses, with mild to moderate additional effects which the subjects expected having prior experience in preliminary trials. This design led to significant physiologic respiratory and subjective changes, which elicited robust signals, inter alia, in primary respiratory structures, which are small. Likewise, our subject selection aimed to reduce any propensity to certain emotional effects (e.g., anxiety).

Mesencephalic and Hypothalamic Effects. The primary contrast (CO₂ FM compared with O₂ FM) showed powerful activations ($Z > 5$) in the midbrain and pons. The loci in the periaqueductal gray are consistent with a powerful state of arousal. The caudal termination of the field of view of the scanner precluded visualization of the rostral ventral respiratory group and the Botzinger complexes. There were major activations in the mesencephalon rostral to these areas, suggesting, within the spatial resolution limitations of PET, possible involvement of the mesencephalic tegmentum, parabrachial nucleus, locus coeruleus, pontine nucleus, and dorsal raphe nucleus (23). Similarly, the posterior hypothalamic activation is consistent with the evidence of local neural mechanisms modulating response to increased PCO₂ (7), and animal studies of c-fos

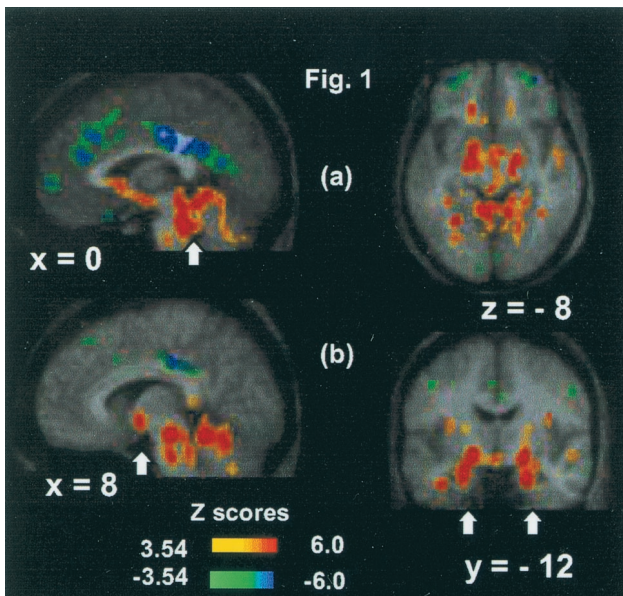


Fig. 1. Activations and deactivations for the CO₂ FM scans compared with the O₂ FM scans displayed on the average MR brain image of the nine subjects. (a) Extensive midbrain and brainstem activations (arrowed) ($x = 0$; $z = -8$), medial frontal and large posterior cingulate deactivations ($x = 0$), and bilateral middle frontal gyri deactivations ($z = -8$). (b) Hypothalamus (arrowed), brainstem, and cerebellum activations ($x = 8$), and highly significant bilateral amygdala activations (arrowed) ($y = -12$). The positive and negative Z -score color coding is shown.

Table 3. Cortical and subcortical activations and deactivations from comparison of the CO₂ FM condition to the O₂ FM, PB, and rest conditions

	BA	CO ₂ FM vs. O ₂ FM					CO ₂ FM vs. PB					CO ₂ FM vs. Rest				
		x	y	z	Size	Z-sc	x	y	z	Size	Z-sc	x	y	z	Size	Z-sc
Activations																
Mesencephalon-diencephalon																
R midbrain tegm		8	-26	-14	125	6.7	8	-28	-12	120	4.1	8	-28	-12	122	4.5
R periacq. gray		2	-34	-12	115	5.4										
R pons		2	-36	-26	125	6.5	12	-36	-26	116	4.8	-10	-38	-28	113	4.4
		6	-28	-30	114	5.4										
R hypothalamus		8	-6	-6	118	5.3	0	-6	-10	123	4.6					
Limbic/paralimbic																
R amygd/ant hipp		21	-12	-22	107	6.9	24	-10	-22	125	5.5	24	-12	-22	121	5.3
L amygd/ant hipp		-20	-12	-18	124	5.9	-22	-12	-18	125	5.1					
R amygd/sublentic		20	-12	-8	120	6.3	20	-10	-10	120	5	20	-12	-8	124	5.5
		16	-16	-14	94	5.9						-16	-10	-8	125	5.9
R amygdala							30	-6	-14	119	5.1	28	-4	-14	112	4.7
R parahipp gyrus	20	32	-4	-34	89	5.4										
	36	32	-18	-24	124	5.4	32	-22	-26	90	4.2					
L parahipp gyrus	36	-34	-12	-26	124	5.1										
R parahipp gyrus/ar	28						18	-18	-18	100	4.8					
L fus gyrus	19	-26	-58	-8	118	6.5										
	37	-32	-44	-10	105	5.3						-32	-46	-10	91	4.0
R fus gyrus	37	40	-42	-12	107	5.4										
L ventr ant cing	24	-14	24	-6	121	5.4	-6	20	-2	103	4.7	-8	28	2	98	4.5
	24						-10	30	6	111	4.7					
R ant insula		32	-2	16	79	5.0						32	8	16	72	4.2
Other																
R pulv		20	-28	4	103	5.8						20	-32	2	98	5.9
R put/caud		22	14	10	119	6.0										
		20	26	0	124	5.5										
L put/caud		-14	12	20	56	5.4										
L caud		-20	18	4	105	5.2						-22	16	8	73	4.1
R mid temp gyrus	21	40	-2	-18	116	5.1	42	-2	-18	124	4.3					
Deactivations																
Dors ant cing	24	4	6	34	118	-6.4	2	22	32	122	-4.8	-2	20	34	100	-5
	24	0	28	18	118	5.5										
Post cing	23	0	-36	32	90	-7.0	0	-26	-32	119	-4.9	0	-26	30	120	-5.5
	23	0	-50	26	95	-5.7	-2	-42	28	104	-4.8	0	-50	22	122	-6.8
	31	1	-62	14	99	-5.1										
R inf front/orb gyrus	47	33	23	-20	74	-6.5	24	32	-12	104	-4.2					
R mid front gyrus	47	32	48	-8	51	-5.5						30	48	-8	61	-5.2
L mid front gyrus	47	-30	48	-6	60	-5.6						-32	47	-8	49	-5.6
	10											-24	50	8	68	-5.2
R orb gyrus	47	-24	20	-26	49	-5.1										
L rect gyrus	11	-2	14	-22	55	-6.0						-1	10	-18	87	-5.3
R mid front gyrus	10	2	52	0	97	-5.2										
R mid front gyrus	8	22	22	38	122	5.5										
L mid front gyrus	9	-24	32	28	118	-5.4	-22	38	30	47	-4.5	-24	20	48	72	-6.0
L mid front gyrus	8	-30	8	44	125	-5.1	-32	8	42	108	-4.1	-30	8	42	112	-5.3
R mid front gyrus	6	26	16	44	109	-5.0	30	18	44	117	-4.2	30	20	44	114	-5.6
R precentr gyrus	4						50	-16	36	120	-5.1					
R precentr gyrus	6						54	-8	11	113	-4.9					
L inf temp gyrus	20											-54	-16	-28	50	-5.3

Regions shown have significance $Z > 5.0$ for the O₂ FM condition, $Z > 4.0$ for the PB and rest conditions, and a large cluster size (voxels > 45 ; voxel volume 8 mm³). The left-hand column (the primary comparison) has BA specified.

response to hypercapnia, which included posterior hypothalamic, paraventricular, and parabrachial nucleus (24).

Limbic and Paralimbic Effects. There was intense activation of the amygdala and periamygdalar region, hippocampi, and parahippocampal gyri, which are phylogenetically ancient brain regions. The rapid chemical changes in the blood perfusing the brainstem entrain a powerful arousal, which is potentially both stressful and

alarming because it parallels a natural circumstance where the organism is imperiled by compromise of air supply. The activation of the amygdala may reflect the strong reciprocal connectivity of this structure with the brainstem mechanisms of arousal and also the respiratory centers. The reciprocal connectivity is indicated both by the autonomic effects of amygdala stimulation in the conscious human, which causes rise in respiration and heart rate, as well as the sense of fear and dread, which occur with amygdala

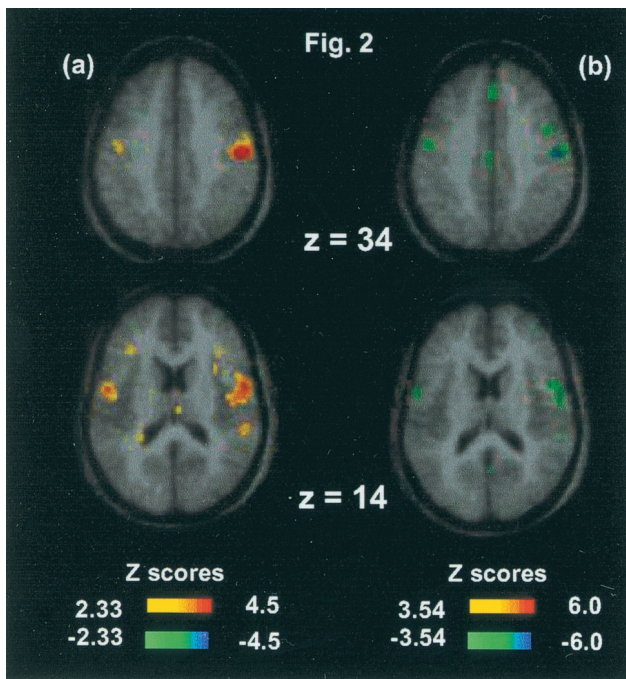


Fig. 2. (a) PB versus rest. Activation of right primary motor cortex ($x = 50, y = -20, z = 36, Z$ score = 4.6) and bilateral inferior premotor cortex ($x = 54, y = -4, z = 14, Z$ score = 3.5; and $x = -48, y = -8, z = 14, Z$ score = 3.4). (b) CO₂ FM versus PB. Relative deactivations in right precentral cortex ($x = 50, y = -16, z = 36, Z$ score = -5.1) and bilateral inferior premotor cortex ($x = 54, y = -8, z = 11, Z$ score = -4.9; and $x = -52, y = -4, z = 16, Z$ score = -4.7). Note the colocalization of the motor-premotor effects of volitional breathing.

stimulation or epilepsy originating in the amygdala (25, 26). There is extensive evidence of the amygdala being a central structure in conditioned fear through many levels of evolutionary development (25). It gives rise to defense, freezing, and escape mechanisms together with autonomic response. Thus, whereas the subjects used here were selected on the basis that they did not admit to significant anxiety in the preliminary trials, nor in these experiments, the data of large amygdala activation with hypercapnic medullary stimulation may reflect both preconscious and conscious detection of threat as considered below.

The contemporaneous major activation of the hippocampi is consistent with activation of memory. Hippocampal memory activation set off by cortical processes and autonomic feedback has been indicted in initiation of panic attacks (25), which also can be initiated by inhalation of CO₂ (27). Lesion of the hippocampus has been shown in animals to disrupt aspects of conditioned fear response as does amygdala lesion (28).

Robust amygdala activity occurs with auditory, olfactory, and gustatory aversive stimuli (29–31) and with faces registering fear that are immediately masked; the latter finding supports a main role in the automatic, preconscious early detection of threat in the environment (32). Animal studies identify multiple routes for CO₂-induced responses in the amygdala, via direct projections from the ventral medulla (6), and indirect pathways through midbrain tegmentum (33), hypothalamus, and thalamic and septal nuclei (34). The amygdala activation could be an important intermediary component in the development of air hunger with anxiety and fear.

Activation of the rostral and ventral portion of the ACC has also not been reported before in association with CO₂ stimulation. This limbic subdivision is segregated from the dorsal ACC subdivision, which subserves cognitive functions (35). The affective portion of the ACC has strong reciprocal connections to amygdala, periaqueductal gray, nucleus accumbens, hypothalamus, anterior insula

and orbitofrontal cortex, and outflow to autonomic, visceromotor and endocrine systems (35) and has been found to be activated by affect-related tasks, including induced sadness in normal individuals and individuals with major depression (36).

Activations in the vicinity of the hippocampus, parahippocampus, and fusiform gyrus confirm similar findings observed in a previous study of CO₂ breathing (11). The fusiform gyrus, traditionally associated with the ventral visual processing stream specialized for object recognition and face processing (37), has been implicated in emotional processing by recent PET and functional MRI studies showing intense fusiform responses to emotion conveyed by face and voice, particularly anxiety (38). The right fusiform activity correlated strongly with amygdala activity during processing of fearful versus other expressions (38).

Motor Effects and Insula. Activation of primary motor cortex BA4 and inferior premotor cortex BA6 was observed in PB versus rest, confirming activity in similar cortical motor areas involved in volitional breathing (9, 10). Importantly, these effects were exactly matched by relative deactivations in the CO₂ FM versus PB comparison. Our field of view precluded the visualization of dorsal motor activations in the proximity of the vertex (9, 10). The absence of motor-premotor activity during all comparisons involving CO₂ FM demonstrates the clear functional segregation of the cortical representation of volitional versus CO₂-stimulated breathing (11).

Activation of the right insula cortex was observed in CO₂ FM versus O₂ FM, and CO₂ FM versus rest, but not in the comparison of CO₂ FM versus PB. Activation of the anterior insular cortex during air hunger was reported before by Corfield *et al.* (11) and Banzett *et al.* (39). The study by Banzett and colleagues (39), however, differs from the one reported here. Their subjects were mechanically ventilated, and the end tidal PCO₂ was held constant at 4 mm Hg above normal in both control and experimental conditions. For the control condition air hunger was relieved by setting the ventilator at a high tidal volume. For the experimental condition, the subjects were ventilated at a tidal volume well below the level of spontaneous respiration at the prevailing arterial PCO₂. The air hunger produced caused a large activation of the insular cortex bilaterally and was associated also with activations in the motor cortex involving the precentral gyrus, the supplementary motor area, the frontal operculum as well as the putamen, albeit some at a level below significance when examining the whole brain. Motor areas also were activated in our PB versus rest comparison (Fig. 2), as in other volitional breathing studies (9, 10). The motor involvement may, as suggested, reflect the conscious suppression of breathing required to cooperate with the mechanical ventilator (39), and thus the frustration of a motor drive. The dominant insular activation is attributed to afferent inflow via the thalamus conveying the air hunger signal (39), although the authors note motor connections do converge on the insula. Correspondingly with our study, the hypercapnia, as contrived experimentally, did cause sensory effects other than air hunger, which may have contributed to elements of the observed regional changes. Air hunger divorced from all other physiological concomitants is unlikely. One method of production parallels respiratory muscle or lung impairment (39), whereas our experiments parallel circumstances such as suffocation including intense crowding of a confined space (burrowing animals) or breath holding under water.

Caudate. The bilateral caudate activations in the comparisons involving CO₂ FM could be consistent with an alerting or priming mechanism for the motor system (40). The limbic lobes project to areas of the motor cortex but also to major subcortical motor structures such as caudate nucleus, putamen (41), and pons.

Cortical Deactivations. An important finding of this study is the strong deactivation of the dorsal segment of the ACC, the posterior cingulate cortex, and the lateral prefrontal cortex (BA46 and BA9)

during hypercapnia and air hunger. The dorsal subdivision of the ACC is part of a distributed attentional network with strong reciprocal connections to lateral prefrontal cortex (BA46/9), parietal cortex (BA7), and posterior cingulate cortex (35) and is consistently activated by cognitively demanding tasks, such as the Stroop test. Decreased rCBF of the dorsal ACC has been reported during intense emotional states, such as memory-driven or film-generated sadness (36) or anticipating pain (40). In the anesthetized cat, electrical stimulation of the amygdala evoked a cough-like spasmodic expiratory response, which was suppressed by concomitant stimulation of the anterior cingulate gyrus or orbital gyrus (42), confirming a top-down inhibitory control by these cortical regions.

gCBF Effects. The issue of gCBF changes confounding rCBF effects is important both in this and other experiments where CO₂, which is known to increase gCBF, is a primary stimulant. We observed gCBF increases of 21% during the CO₂ conditions compared with the resting gCBF and a decrease of 19% during the PB condition. The global normalization procedures used in this PET activation study removed the gCBF changes when analyzing for rCBF differences. Previous work involving visual stimulation and activation of occipital cortex has demonstrated that gCBF changes in PET activation studies do not preclude identification of significant rCBF changes (11). The majority of rCBF changes identified in our primary contrast (CO₂ FM compared with O₂ FM) also were observed in the CO₂ FM comparison with PB. This is despite a 40%

gCBF difference existing between the CO₂ FM and PB conditions and a 26% gCBF difference between the CO₂ FM and O₂ FM conditions.

Conclusions

In summary, the striking response of limbic and paralimbic regions to CO₂ stimulation points to these structures having a singular role in the affective sequelae entrained by disturbance of basic respiratory control whereby a process of which we are normally unaware becomes the salient element of consciousness. We propose that rostral and ventral ACC, hippocampus and parahippocampus, amygdala, insula and fusiform gyrus, along with deactivations in dorsal anterior and posterior cingulate and prefrontal cortex represent a distributed network involved in the affective representation and/or regulation of breathing. Their dysregulation may play a role in the breathing abnormalities observed in panic disorder (1) as well as other emotional disorders.

We gratefully acknowledge helpful comments from George Paxinos, Simon Gandevia, John Watson, John R. Pappenheimier, Helen S. Mayberg, Robin McAllen, and Per Roland. This work has been supported by the benefactors of the Research Imaging Center, San Antonio, the National Health and Medical Research Council of Australia, the Howard Florey Biomedical Foundation of the United States, the Harold G. and Leila Y. Mathers Charitable Foundation, and the Robert J. Jr. and Helen C. Kleberg Foundation.

- Klein, D. F. (1993) *Arch. Gen. Psychiatry*, **50**, 306–317.
- Pappenheimier, J. R. (1965) *Harvey Lect.* **61**, 71–94.
- Banzett, R. B., Lansing, R. W., Reid, M. B., Adams, L. & Brown, R. (1989) *Respir. Physiol.* **76**, 53–67.
- Banzett, R. B., Lansing, R. W., Karleyton, C. E. & Shea, S. E. (1996) *Respir. Physiol.* **103**, 19–31.
- Gandevia, S. C., Killean, K., McKenzie, D. K., Crawford, M., Allen, G. M., Gorman, R. B. & Hales, J. P. (1993) *J. Physiol. (London)* **470**, 85–107.
- Gaytan, S. P. & Pasaro, R. (1998) *Brain Res.* **47**, 625–642.
- Horn, E. M. & Waldrop, T. G. (1998) *Respir. Physiol.* **114**, 201–211.
- Gozal, D., Hathout, G. M., Kirlaw, K. A. T., Tang, H., Wood, M. S., Zhang, J., Lufkin, R. B. & Harper, R. M. (1994) *J. Appl. Physiol.* **76**, 2076–2083.
- Colebatch, J. G., Adams, L., Murphy, K., Martin, A. J., Lammertsma, A. A., Tochon-Danguy, H. J., Clark, J. C., Friston, K. J. & Guz, A. (1991) *J. Physiol. (London)* **443**, 91–103.
- Ramsay, S. C., Adams, L., Murphy, K., Corfield, D. R., Grootoonk, S., Bailey, D. L., Frackowiak, R. S. J. & Guz, A. (1993) *J. Physiol. (London)* **461**, 85–101.
- Corfield, D. R., Fink, G. R., Ramsay, S. C., Murphy, K., Harty, H. R., Watson, J. D. G., Adams, L., Frackowiak, R. S. J. & Guz, A. (1995) *J. Physiol. (London)* **488**, 71–84.
- Guz, A. (1997) *Respir. Physiol.* **109**, 197–204.
- Fox, P. T., Perlmutter, J. S. & Raichle, M. E. (1985) *Comput. Assist. Tomogr.* **9**, 141–153.
- Raichle, M. E., Martin, W., Herscovitch, P., Mintun, M. A. & Markham, J. (1983) *J. Nucl. Med.* **24**, 790–798.
- Fox, P. T. & Mintun, M. A. (1988) *J. Nucl. Med.* **30**, 141–149.
- Lancaster, J. L., Glass, T. G., Lakipalli, B. R., Downs, R., Mayberg, H. & Fox, P. T. (1995) *Hum. Brain Mapp.* **3**, 209–223.
- Talairach, J. & Tournoux, P. (1988) *Coplanar Stereotaxic Atlas of the Human Brain* (Verlag, New York).
- Fox, P. T., Mintun, M. A., Reiman, E. M. & Raichle, M. E. (1989) *J. Cereb. Blood Flow Metab.* **9**, 96–103.
- Mintun, M. A., Fox, P. T. & Raichle, M. E. (1989) *J. Cereb. Blood Flow Metab.* **9**, 96–103.
- Worsley, K. J., Evans, A. C., Marrett, S. & Neelin, A. (1992) *J. Cereb. Blood Flow Metab.* **12**, 900–918.
- D'Agostino, R. B., Belanger, A. & D'Agostino, R. B., Jr. (1990) *Am. Stat.* **44**, 316–321.
- Lancaster, J. L., Rainey, L. H., Summerlin, J. L., Freitas, C. S., Fox, P. T., Evans, A. F., Toga, A. W. & Mazziotta, J. C. (1997) *Hum. Brain Mapp.* **5**, 238–242.
- Paxinos, G. & Huang, X. (1995) *Atlas of the Human Brain Stem* (Academic, San Diego).
- Berquin, P., Bodineaux, L., Gross, F. & Larnicol, N. (2000) *Brain Res.* **857**, 30–40.
- Le Doux, J. (1998) *The Emotional Brain* (Simon & Schuster, New York).
- Damasio, A. (1999) *The Feeling of What Happens* (Heinemann, London).
- Margraf, J., Ehlers, A. W. & Roth, W. T. (1986) *Behav. Res. Ther.* **24**, 553–567.
- Kapp, B. S., Wilson, A., Pascoe, J., Supple, W. & Whelan, P. J. (1990) in *Learning and Computational Neuroscience: Foundations of Adaptive Networks*, eds. Gabriel, M. & Moore, J. (MIT Press, Cambridge, MA), pp. 53–90.
- Buchel, C., Dolan, R. J., Armony, J. L. & Friston, K. J. (1999) *J. Neurosci.* **19**, 10869–10876.
- Zald, D. H. & Pardo, J. V. (1997) *Proc. Natl. Acad. Sci. USA* **94**, 4119–4124.
- Zald, D. H., Lee, J. T., Fluegel, K. W. & Pardo, J. V. (1998) *Brain* **121**, 1143–1154.
- Morris, J. S., Ohman, A. & Dolan, R. J. (1999) *Proc. Natl. Acad. Sci. USA* **96**, 1680–1685.
- Walker, D. L., Cassella, J. V., Lee, Y., De Lima, T. C. & Davis, M. (1997) *Neurosci. Biobehav. Rev.* **21**, 743–753.
- Kanemaru, H., Nakamura, H., Isayama, H., Kawabuchi, M. & Tashiro, N. (2000) *Brain Res. Bull.* **51**, 219–232.
- Vogt, B. A., Nimchinsky, E. A., Vogt, L. J. & Hof, P. R. (1995) *J. Comp. Neurol.* **359**, 490–506.
- Liotti, M., Mayberg, H. S., Brannan, S. K., McGinnis, S., Jerabek P. & Fox, P. T. (2000) *Biol. Psychiatry* **48**, 30–42.
- Haxby, J. V., Grady, C. L., Horwitz, B., Ungerleider, L. G., Mishkin, M., Carson, R. E., Herscovitch, P., Schapiro, M. B. & Rapoport, S. I. (1991) *Proc. Natl. Acad. Sci. USA* **88**, 1621–1625.
- Morris, J. S., Friston, K. J., Buchel, C., Frith, C. D., Young, A. W., Calder, A. J. & Dolan, R. J. (1998) *Brain* **121**, 47–57.
- Banzett, R. B., Mulnier, H. E., Murphy, K., Rosen, S. D., Wise, R. J. & Adams, L. (2000) *NeuroReport* **11**, 2117–2120.
- Jones, A. K. P., Brown, W. D., Friston, K. J., Qi, L. Y. & Frackowiak, R. S. J. (1991) *Proc. R. Soc. London Ser. B* **244**, 39–44.
- Van Hoesen, G. W., Yeterian, E. H. & Lavizza-Mourey, R. (1981) *J. Comp. Neurol.* **199**, 205–219.
- Kase, Y., Kito, G., Miyata, T. & Takahama, K. (1984) *Brain Res.* **306**, 293–298.